Response to Referee #1

We thank the reviewer for his/her time and consideration, and for the constructive comments. We are confident that all remarks have been carefully addressed and that the manuscript has been improved accordingly. Our point-by-point response is provided below (text in italics denotes excerpts from the revised manuscript).

Referee's comment 1. Diémoz et al. presents a new PM10 source apportionment framework, RASPBERRY, based on aerosol physical properties derived from OPC and aethalometer measurements. By comparison with chemical PMF results, the authors showed the clear strengths of RASPBERRY. The manuscript is well organized and easy to follow. However, I still have some issues before the manuscript can be accepted. Line 292, the authors mentioned "heuristic uncertainty" was optimized through trial-error methods or iterative approach. Given the strong influence of uncertainty definition of PMF outcomes, can authors provide more details how to derive this parameterization to ensure the reproductivity?

Author's response 1. We thank the reviewer for the positive overall assessment and for raising the point of the limited level of detail originally provided to describe the uncertainty configuration in our approach. Indeed, RASPBERRY reproductivity is actually a goal of this work. To address this potential shortcoming, while at the same time keeping the main text concise, we expanded Sect. S7 of the Supplement. In particular, we now provide a complete description of the procedure used to determine the optimal uncertainty configuration. This workflow is presented in an objective and reproducible manner. We also removed the term 'heuristic', which – although commonly used in the PMF literature – may give the misleading impression that the parameter selection was excessively subjective or arbitrary.

The revised text reads:

The uncertainty framework employed in this study follows the methodology outlined by Vörösmarty et al. (2024), in which the PMF input uncertainty is parametrised as in Eqs. (4) and (5) of the main text. This formulation essentially represents a semi-empirical error model, with notation likely inherited from earlier PMF implementations (PMF2), and separates the uncertainty into two components representing common sources of uncertainty in aerosol measurements: (i) baseline instrument/analysis noise, ensuring a minimum uncertainty even when concentrations are small; and (ii) a concentration-dependent error, which increases proportionally with the measured concentration. The interested reader is referred to that work, and the references therein, for further details. Here we instead present an objective and reproducible workflow describing, step by step, how the free coefficients A, α, and C_3 were selected:

1. *Choice for A and α started from relevant ranges suggested in the aforementioned study and in the scientific literature (e.g., Zhou et al., 2005a; Ogulei et al., 2006, 2007; Gu et al., 2011), i.e. 0.01 to 0.05*

for the product $A \times \alpha$. In our case, $A = 1$ was assigned to size channels and optical absorption, and $\alpha = 0.01$ was used as an initial value, following Vörösmarty et al. (2024).

2. *Choice for C_3 started from values between 0.01 and 0.5. For example, Vörösmarty et al. (2024) select 0.10 for most of their channels. A value of 10 % represents a reasonable a priori estimate of the uncertainty when no additional information is available, therefore C_3 was initially set to this value in our case.*

3. *We then ensured that the total variable (e.g., PM_{10}) did not influence the factorisation by setting it as 'weak' in the PMF (or by assigning $A = 3$ and $C_3' = C_3 \times 3$).*

4. *An initial PMF run was performed, and the residual distribution (Q/Q_{exp}) for each 'species' (VSD channels from OPC and aethalometer spectral absorption at the measured wavelengths) was recorded. At this stage, the volume distribution component typically dominated the profile splitting and was better reproduced by the PMF, with the exception of the largest size ranges (as also reported by Vörösmarty et al., 2024), whereas spectral absorption contributed only marginally to the separation and was not well reproduced (resulting in a high Q/Q_{exp} ratio). This behaviour arises from the larger number of 'channels' associated with particle size (OPC measurements) compared with those related to multispectral optical absorption (aethalometer). This imbalance was corrected in the subsequent steps.*

5. *We gradually adjusted the uncertainty until three criteria were simultaneously satisfied: (i) the factor contributions remained as uncorrelated as possible; (ii) the scaled residuals fell within the expected range (± 3, Norris et al., 2014); and (iii) the resulting profiles and contributions were physically plausible.*

6. *In our case, reducing the residuals (and the Q/Q_{exp} ratio) for the largest size channels without artificially splitting the coarse 'local resuspension' factor into two modes required increasing their uncertainty. This resulted in $C_3 = 0.3$ for size channels with particles larger than $2\,\mu m$ and $C_3 = 0.4$ for particles above $6\,\mu m$. The $2\,\mu m$ and $6\,\mu m$ thresholds were selected as representative of the desert dust and coarse resuspension modes, based on previous literature (see main text) and the examination of the temporal evolution of the volume size distributions. Indeed, these C_3 values improved the separation between desert dust and local resuspension contributions. Larger uncertainty values tended to merge these contributions, whereas smaller values tended to split the local resuspension factor into multiple modes.*

7. *Conversely, in order for the absorption measurements to contribute effectively to shaping the factor profiles, their uncertainty had to be reduced. In this study, C_3 was set to 0.05 for aethalometer measurements. Using higher values caused the size-related portion of the PMF to dominate due to the larger number of size classes, leading to additional size modes lacking clear physical interpretation. In some configurations, the contributions associated with traffic emissions and residential biomass burning became unrealistically small. Similar issues concerning the mass of the traffic factor were reported by Forello et al. (2023). Notably, the selected configuration yielded PM_{10} contributions for traffic and biomass burning that are consistent with the method described by Aujay-Plouzeau (2020), which is based solely on aethalometer measurements.*

8. *During this process, it was necessary to increase the number of factors relative to the initial run, which was based only on size, in order to accommodate factors emerging from the multispectral absorption-driven splitting (e.g., traffic, biomass burning, condensation-mode secondary aerosols). More details on the selection of the optimal number of factors are provided in Sect. S11.*

9. *The plot of the original and reconstructed time series were examined for each input species to verify whether the selected uncertainty configuration reproduced the original data satisfactorily.*

10. *Note that α primarily affects the PMF behaviour at low concentrations of a species, whereas C_3 influences the behaviour at medium to high concentrations. This distinction is particularly important for species exhibiting a marked seasonal cycle, such as those related to biomass burning. In such cases, the minimum uncertainty (constant component, see Table S1) should be chosen so that winter and summer conditions are clearly distinguished, i.e. situations in which the species is present or absent in the atmosphere are well separated.*

11. *The factor uncertainties were finely adjusted at the end of the procedure by scaling them so that the residuals fell within the expected range of* ± 3. *In this study, an additional 20 % increase in all* C_3 *values was required. The coefficients were scaled accordingly rather than introducing an additional parameter ('Additional model uncertainty') in EPA PMF 5.0. The* C_3 *values reported in Table S1 include this factor and their reported digits are approximated to* ± 0.05 *for clarity.*

The final values for the parameters A, α*, and* C_3 *are shown in Table S1. [...]*

It may be noted that:

- *The uncertainty assigned to the largest size channels (*$d > 6\,\mu m$*) is relatively high. This reflects the low number concentration of large particles and their 'shot' nature, which introduces greater variability when considered from a Poisson-based perspective (Sect. S2.1). Indeed, these bins typically contain a few peak values emerging from a background of zeros, whose frequency can reach up to 30 %. Consequently, these size channels, together with the total variable* PM_{10}*, were classified as weak variables in the PMF configuration to prevent them from exerting excessive influence during subsequent tests. During the testing phase, as suggested in previous studies (e.g., Zhou et al., 2004; Thimmaiah et al., 2009; Zhou et al., 2005b), an alternative approach was also evaluated in which the largest size bins were grouped (in sets of three to five, depending on particle size) to mitigate issues associated with low particle counts and to improve the signal-to-noise ratio (SNR). Although bin grouping effectively increased the SNR, it hindered the separation of the two coarse factors (desert dust and local resuspension). For this reason, this approach was not adopted in the final configuration.*
- *The NeBC uncertainties used in this study are lower than those reported in some previous works (e.g., Forello et al., 2019; Rigler et al., 2020). In particular, Forello et al. (2023) applied an uncertainty as high as 50 % for* b_{abs} *to avoid convergence issues when coupling absorption data with chemical data in the PMF. With such high uncertainty values, combined with the smaller number of optical variables relative to chemical species, the NeBC information effectively follows the factorisation rather than contributing to it. In contrast, the present approach aims to ensure that both spectral absorption and volume size distribution contribute to determining the final solution. Consequently, the uncertainty values adopted here should not be interpreted as strict measurement uncertainties, but rather as weighting parameters used to balance the influence of the different input variables on the Q metric.*

RC2. For traffic emissions between chemical and physical PMF results, their correlation is not that high, r2=0.45. The authors attributed to the detection limit of OPC. Is it possible to improve the physical PMF by introducing other factors, such as NOx?

AR2. We thank the reviewer for this comment, which allowed us to clarify the reasons why NO_x were not included in the PMF. More specifically, we introduced the following section in the Supplement (Sect. S5: On the inclusion of gases in the physical PMF):

Recent guidelines of the European project RI-URBANS (Petit et al., 2024) also suggest including NO_x *in PMF analyses. This practice may be useful for supporting the factor-source attribution based on the factor* NO_x *is associated with. In such cases,* NO_x *should be introduced into the PMF as weak species (e.g., Vörösmarty et al., 2024) in order to prevent them from exerting an excessive influence on the separation of the factors (see below).*

However, it should be considered that in Alpine environments, particularly during winter, NO_x *does not exclusively trace traffic emissions but also biomass combustion, and that Aosta is a relatively small, low-traffic city (33,000 inhabitants; Diémoz et al., 2019, 2020, 2021). In the chemical PMF, for example, the*

correlation of NO, NO_2, and NO_x with the biomass-burning factor is higher (R^2 = 0.63, 0.63, and 0.67, respectively) than with the traffic factor (R^2 = 0.56, 0.45, and 0.53).

For this reason, we were cautious about using NO_x as a strong species contributing to the separation of the factors. Several tests performed during the development of this work indicate that, when NO_x is introduced as a strong species, the agreement between the chemical and physical PMF deteriorates and, in some cases, the physical PMF yields unrealistic solutions. For example:

- *When NO_x is introduced with an uncertainty of 5–10 %, the seasonal cycle of NO_x is poorly reproduced by the PMF, with NO being strongly underestimated during winter.*
- *When the uncertainty assigned to NO_x is reduced, both NO and NO_2 are forced to be reproduced more accurately. However, the reconstruction of DeltaC deteriorates ($Q/Q_{exp} = 20$), and the contributions of PM_{bb} and PM_{ff} decrease by approximately a factor of three (i.e., to ~3 %). In some configurations, an additional NO-rich factor separates from the factor associated with traffic emissions.*

This behaviour is likely related to the fact that the relationship between NO_x and aerosol, as also discussed by Rivas et al. (2020), depends on several factors: (a) meteorology and atmospheric dynamics (e.g. solar radiation availability, temperature, etc.); (b) long-term changes in the vehicle fleet; and (c) driving conditions. Consequently, the ratio between NO_x and traffic-related PM can vary throughout the day, between seasons, and over longer time scales as the ones addressed here. In addition, if as we expect the exhaust fraction is not fully captured by the OPC and the PMF is forced to maintain a strong correlation with NO_x, the model may compensate this constraint by reducing the PM_{10} mass attributed to traffic.

Moreover, taking the suggestions received in the review process into account, we introduced the calculation of the uncertainties of the factor contributions (matrix G) for each retrieval using the Effective Variance Least Squares (EVLS) method coupled to the chemical PMF and RASPBERRY. With respect to the traffic factor, this analysis clearly shows that traffic is the factor associated with the largest relative uncertainties, both in the chemical PMF and in RASPBERRY+EVLS. This combination of low signal and comparatively large uncertainty naturally leads to a substantial dispersion in the point-to-point comparison (Fig. 1 here, complementing the results in Fig. 8b reported in the first version of the manuscript and now included in Fig. S34).

We included this discussion in the revised manuscript, and the corresponding paragraph in Sect. 4.3 was therefore updated as follows:

The comparison of traffic factors is depicted in Figs. 8a (time series) and 8b (scatter plot). From the first panel, it is evident that the magnitude of contributions from both source apportionments is about the same, as are the overall seasonal trends. However, the point-to-point relationship illustrated in the second panel reveals some discrepancies, with a Pearson's correlation coefficient of $\rho = 0.67$ (R^2 = 0.45). Furthermore, the regression coefficients deviate from the 1:1 line ($y = 0.58\,x + 0.72\ \mu g\,m^{-3}$). This deviation can be attributed to difficulties in accurately identifying the traffic factor, primarily due to the following reasons:

- *Contributions from both source apportionments are relatively low, steadily remaining below 6 $\mu g\,m^{-3}$, which is consistent with the fact that Aosta is a relatively small, low-traffic city (33,000 inhabitants; Diémoz et al., 2019, 2020, 2021). At the same time, the relative uncertainty associated with traffic emissions is among the highest of all dimensional profiles. This is evident from both the large interval ratio obtained from the DISP test (Sect. 4.2 and Fig. 3) and from the uncertainties derived using the EVLS method for both the physical and the chemical data sets (Fig. S34).*
- *The finite lower detection limit of the OPC does not allow all aerosols emitted by traffic to be captured. In particular, most of the studies focusing on ultrafine and accumulation-mode particles (among the most recent examples, Harni et al., 2024; Beddows et al., 2025; Ćirović et al., 2026; Mapelli et al., 2026) identified at least two distinct factors related to traffic (e.g., freshly nucleated vs more aged or distant particles, or gasoline vs diesel/heavy-duty emissions). This may indicate that the physical setup and the chemical analyses effectively 'detect' different factors attributed to traffic.*

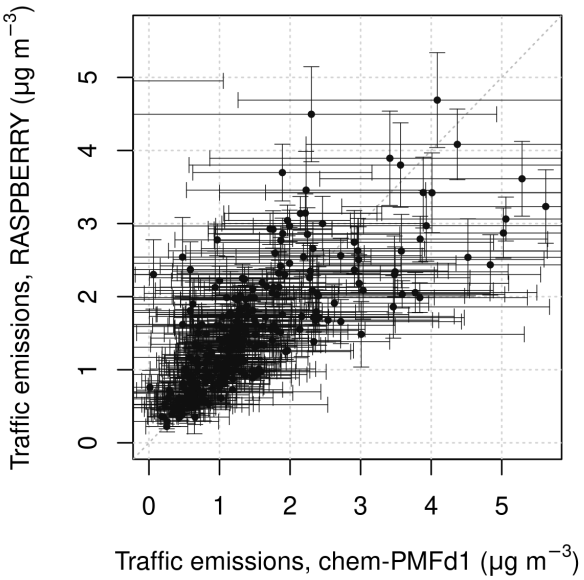

Figure 1: Comparison of daily-averaged PM_{10} source contributions attributed to traffic derived from the chemical PMF (further reprocessed using EVLS) and RASPBERRY+EVLS, shown together with their individual uncertainties. The figure clearly shows that the uncertainty in the chemical source apportionment is larger than in the physical one.

- *The coarse resuspended fraction, which significantly contributes to the mass, may be characterised in slightly different amounts in the chemical and the physical source apportionments, as discussed in Sect. S10. Distinguishing unambiguously exhaust and non-exhaust particle contributions is a well-known challenge, frequently reported in the literature (Forello et al., 2023).*
- *The mass absorption cross-section (MAC) in aethalometer measurements may decrease in winter compared to summer, as observed in several studies, e.g. Mousavi et al. (2019) in Milan and Savadkoohi et al. (2024) on a European scale. Such seasonal variation is consistent with an underestimation of NeBC during winter, when concentrations are higher, and an overestimation during summer, when concentrations are lower, in RASPBERRY.*

At the same time, it should be noted that the comparison slope for the traffic factor is higher than 1 when using York and log-transformed York regressions (Table S3), since the intercept decreases. Therefore, the deviation from the 1:1 line may also be partly attributable to an artefact of the regression method itself.

RC3. The authors also mentioned RASPBERRY improves the efficiency of PMF. How much faster is RASPBERRY is compared to a normal PMF? Can we also apply RASPBERY to the chemical PMF? If so, it would be helpful to discuss whether and how the results would differ from those obtained using a normal chemical PMF approach.

AR3. As shown in Fig. S7, when RASPBERRY retrievals are performed on the same input data, and using the same uncertainties/profiles from the training phase (PMF), the contributions from RASPBERRY and the 'standard' PMF are equivalent. This follows from the fact that the same metric is minimised during both the training and the retrieval phases (Eq. 3), regardless of the dataset used. In principle, the same methodology could also be applied to chemical datasets, in a way conceptually similar to what is commonly known in the literature as the Chemical Mass Balance (CMB) approach. It should also be noted

that, for source apportionment based on online aerosol chemical characterisation measurements, more sophisticated tools than RASPBERRY are available, such as SoFi (Canonaco et al., 2013).

The retrieval phase of RASPBERRY is typically one to two orders of magnitude faster than the PMF training phase for the same number of observations. However, since chemical analyses are generally performed offline on daily samples, the number of data points to be processed is usually much smaller than for physical measurements, which are typically automatic and collected at high time resolution. Consequently, from the perspective of data volume, the computational advantage of applying RASPBERRY to chemical datasets would likely be smaller than that demonstrated in this work for physical measurements. Conversely, once the training phase has been completed, RASPBERRY can be applied to real-time physics-based measurements, enabling rapid source apportionment while avoiding delays associated with PM sampling and chemical analyses, as well as the need to collect sufficiently long-term datasets to perform a chemical PMF. Therefore, RASPBERRY allows environmental agencies to conduct high temporal resolution, real-time, continuous, and cost-effective aerosol source apportionment, while also supporting emergency management.

References

Aujay-Plouzeau, R.: Guide méthodologique pour la mesure du «Black Carbon» par Aethalomètre multi longueur d'onde AE33 dans l'air ambiant (Version 2020), Tech. rep., Ineris, https://www.lcsqa.org/system/files/media/documents/LCSQA2019-Guide_mesure_BlackCarbon_par_AE33_VF03-Approuv%C3%A9CPS15122020.pdf, 2020.

Beddows, D., Brean, J., Rowell, A., Merkel, M., Weinhold, K., Dall'Osto, M., and Harrison, R.: Wide-Positive Matrix Factorisation of particle number size distributions: A new approach accounting for cyclically changing source profiles, Sci. Total Environ., 998, 180 231, https://doi.org/10.1016/j.scitotenv.2025.180231, 2025.

Canonaco, F., Crippa, M., Slowik, J. G., Baltensperger, U., and Prévôt, A. S. H.: SoFi, an IGOR-based interface for the efficient use of the generalized multilinear engine (ME-2) for the source apportionment: ME-2 application to aerosol mass spectrometer data, Atmos. Meas. Tech., 6, 3649–3661, https://doi.org/10.5194/amt-6-3649-2013, 2013.

Ćirović, Ž., Stojanović, D. B., Davidović, M., Onjia, A., Alastuey, A., and Jovašević-Stojanović, M.: New Particle Formation and Source Apportionment of Particle Number Size Distribution in the Urban Area of the City of Belgrade, Atmosphere, 17, https://doi.org/10.3390/atmos17020205, 2026.

Diémoz, H., Gobbi, G. P., Magri, T., Pession, G., Pittavino, S., Tombolato, I. K. F., Campanelli, M., and Barnaba, F.: Transport of Po Valley aerosol pollution to the northwestern Alps – Part 2: Long-term impact on air quality, Atmos. Chem. Phys., 19, 10 129–10 160, https://doi.org/10.5194/acp-19-10129-2019, 2019.

Diémoz, H., Tombolato, I. K. F., Zublena, M., Magri, T., and Ferrero, L.: The impact of biomass burning emissions on PM concentration in the Greater Alpine region, in: Proceedings of 12th International Conference on Air Quality, Science and Application, p. 26, Hatfield, UK, 10.18745/pb.22217, 2020.

Diémoz, H., Magri, T., Pession, G., Tarricone, C., Tombolato, I. K. F., Fasano, G., and Zublena, M.: Air Quality in the Italian Northwestern Alps during Year 2020: Assessment of the COVID-19 «Lockdown Effect» from Multi-Technique Observations and Models, Atmosphere, 12, https://doi.org/10.3390/atmos12081006, 2021.

Forello, A. C., Bernardoni, V., Calzolai, G., Lucarelli, F., Massabò, D., Nava, S., Pileci, R. E., Prati, P., Valentini, S., Valli, G., and Vecchi, R.: Exploiting multi-wavelength aerosol absorption coefficients in a multi-time resolution source apportionment study to retrieve source-dependent absorption parameters, Atmos. Chem. Phys., 19, 11 235–11 252, https://doi.org/10.5194/acp-19-11235-2019, 2019.

Forello, A. C., Cunha-Lopes, I., Almeida, S. M., Alves, C. A., Tchepel, O., Crova, F., and Vecchi, R.: Insights on the combination of off-line and on-line measurement approaches for source apportionment studies, Sci. Total Environ., 900, 165 860, https://doi.org/10.1016/j.scitotenv.2023.165860, 2023.

Gu, J., Pitz, M., Schnelle-Kreis, J., Diemer, J., Reller, A., Zimmermann, R., Soentgen, J., Stoelzel, M., Wichmann, H.-E., Peters, A., and Cyrys, J.: Source apportionment of ambient particles: Comparison of positive matrix factorization analysis applied to particle size distribution and chemical composition data, Atmos. Environ., 45, 1849–1857, https://doi.org/10.1016/j.atmosenv.2011.01.009, 2011.

Harni, S. D., Aurela, M., Saarikoski, S., Niemi, J. V., Portin, H., Manninen, H., Leinonen, V., Aalto, P., Hopke, P. K., Petäjä, T., Rönkkö, T., and Timonen, H.: Source apportionment of particle number size distribution at the street canyon and urban background sites, Atmos. Chem. Phys., 24, 12 143–12 160, https://doi.org/10.5194/acp-24-12143-2024, 2024.

Mapelli, C., Diémoz, H., Contini, D., Dinoi, A., Cesari, D., and Barnaba, F.: Physics-based aerosol source apportionment at the site of Lecce (Italy), Atmos. Res. (under review), 2026.

Mousavi, A., Sowlat, M. H., Lovett, C., Rauber, M., Szidat, S., Boffi, R., Borgini, A., De Marco, C., Ruprecht, A. A., and Sioutas, C.: Source apportionment of black carbon (BC) from fossil fuel and biomass burning in metropolitan Milan, Italy, Atmos. Environ., 203, 252–261, https://doi.org/10.1016/j.atmosenv.2019.02.009, 2019.

Norris, G., Duvall, R., and Brown, S.: EPA Positive Matrix Factorization (PMF) 5.0 Fundamentals and User Guide, U.S. Environmental Protection Agency Office of Research and Development Washington, DC 20460, `https://www.epa.gov/sites/default/files/2015-02/documents/pmf_5.0_user_guide.pdf`, ePA/600/R-14/108, 2014.

Ogulei, D., Hopke, P. K., Zhou, L., Pancras, J. P., Nair, N., and Ondov, J. M.: Source apportionment of Baltimore aerosol from combined size distribution and chemical composition data, Atmos. Environ., 40, 396–410, https://doi.org/10.1016/j.atmosenv.2005.11.075, 2006.

Ogulei, D., Hopke, P. K., Chalupa, D. C., , and Utell, M. J.: Modeling Source Contributions to Submicron Particle Number Concentrations Measured in Rochester, New York, Aerosol Sci. Tech., 41, 179–201, https://doi.org/10.1080/02786820601116012, 2007.

Petit, J.-E., Favez, O., and Chauvigné, A.: Deliverable D5 (D1.5) NRT Source Apportionment Service Tools for submicron carbonaceous matter (final), Tech. rep., RI-URBANS Research Infrastructures Services Reinforcing Air Quality Monitoring Capacities in European Urban & Industrial AreaS (GA n. 101036245), `https://riurbans.eu/wp-content/uploads/2024/12/RI-URBANS_D5_D1_5.pdf`, 2024.

Rigler, M., Drinovec, L., Lavrič, G., Vlachou, A., Prévôt, A. S. H., Jaffrezo, J. L., Stavroulas, I., Sciare, J., Burger, J., Kranjc, I., Turšič, J., Hansen, A. D. A., and Močnik, G.: The new instrument using a TC–BC (total carbon–black carbon) method for the online measurement of carbonaceous aerosols, Atmos. Meas. Tech., 13, 4333–4351, https://doi.org/10.5194/amt-13-4333-2020, 2020.

Rivas, I., Beddows, D. C., Amato, F., Green, D. C., Järvi, L., Hueglin, C., Reche, C., Timonen, H., Fuller, G. W., Niemi, J. V., Pérez, N., Aurela, M., Hopke, P. K., Alastuey, A., Kulmala, M., Harrison, R. M., Querol, X., and Kelly, F. J.: Source apportionment of particle number size distribution in urban background and traffic stations in four European cities, Environ. Int., 135, 105 345, https://doi.org/10.1016/j.envint.2019.105345, 2020.

Savadkoohi, M., Pandolfi, M., Favez, O., Putaud, J.-P., Eleftheriadis, K., Fiebig, M., Hopke, P. K., Laj, P., Wiedensohler, A., Alados-Arboledas, L., Bastian, S., Chazeau, B., Álvaro Clemente María, Colombi, C., Costabile, F., Green, D. C., Hueglin, C., Liakakou, E., Luoma, K., Listrani, S., Mihalopoulos, N., Marchand, N., Močnik, G., Niemi, J. V., Ondráček, J., Petit, J.-E., Rattigan, O. V., Reche, C., Timonen, H., Titos, G., Tremper, A. H., Vratolis, S., Vodička, P., Funes, E. Y., Zíková, N., Harrison, R. M., Petäjä, T., Alastuey, A., and Querol, X.: Recommendations for reporting equivalent black carbon (eBC) mass concentrations based on long-term pan-European in-situ observations, Environ. Int., 185, 108 553, https://doi.org/10.1016/j.envint.2024.108553, 2024.

Thimmaiah, D., Hovorka, J., and Hopke, P. K.: Source apportionment of winter submicron prague aerosols from combined particle number size distribution and gaseous composition data, Aerosol Air Qual. Res., 9, 209–236, https://doi.org/10.4209/aaqr.2008.11.0055, 2009.

Vörösmarty, M., Hopke, P. K., and Salma, I.: Attribution of aerosol particle number size distributions to main sources using an 11-year urban dataset, Atmos. Chem. Phys., 24, 5695–5712, https://doi.org/10.5194/acp-24-5695-2024, 2024.

Zhou, L., Hopke, P. K., Paatero, P., Ondov, J. M., Pancras, J., Pekney, N. J., and Davidson, C. I.: Advanced factor analysis for multiple time resolution aerosol composition data, Atmos. Environ., 38, 4909–4920, https://doi.org/10.1016/j.atmosenv.2004.05.040, 2004.

Zhou, L., Hopke, P. K., Stanier, C. O., Pandis, S. N., Ondov, J. M., and Pancras, J. P.: Investigation of the relationship between chemical composition and size distribution of airborne particles by partial least squares and positive matrix factorization, J. Geophys. Res., 110, https://doi.org/10.1029/2004JD005050, 2005a.

Zhou, L., Kim, E., Hopke, P. K., Stanier, C., and Pandis, S. N.: Mining airborne particulate size distribution data by positive matrix factorization, J. Geophys. Res., 110, https://doi.org/10.1029/2004JD004707, 2005b.